

We are IntechOpen, the world's leading publisher of Open Access books Built by scientists, for scientists

6,900

Open access books available

185,000

International authors and editors

200M

Downloads

Our authors are among the

154

Countries delivered to

TOP 1%

most cited scientists

12.2%

Contributors from top 500 universities



WEB OF SCIENCE™

Selection of our books indexed in the Book Citation Index
in Web of Science™ Core Collection (BKCI)

Interested in publishing with us?
Contact book.department@intechopen.com

Numbers displayed above are based on latest data collected.
For more information visit www.intechopen.com



Application of Multi-Walled Carbon Nanotubes for Innovation in Advanced Refractories

Yawei Li¹, C.G. Aneziris², Shengli Jin¹, Shaobai Sang¹ and Xilai Chen¹

¹Wuhan University of Science and Technology

²Technische Universität Bergakademie Freiberg

¹P. R. China

²Germany

1. Introduction

Carbon nanotubes (CNTs) have attracted extensively interest of scientists and engineers due to their outstanding physical properties such as low density, high aspect ratio, Young's modulus, electrical and thermal conductivities. When single-wall carbon nanotubes (SWCNTs) or multi-wall carbon nanotubes (MWCNTs) are introduced into ceramics, metals and polymers as matrices, ultra-high strength and/or multifunctional composites can be developed as expected. Recently, CNT composite refractories have been the subject of intense research activities. In this chapter, MWCNTs (hereafter named as CNTs) were introduced into refractories to improve their mechanical properties and thermal conductivity, such as Al₂O₃-C refractories for slide gates and carbon blocks for blast furnaces in iron and steel making industry.

2. Application of CNTs in Al₂O₃-C refractories

2.1 Experimental procedure

Tabular alumina (8-14 mesh, -14 mesh and -325 mesh, 99.5 -wt% Al₂O₃, Almatis), reactive alumina (d₅₀ = 5 μm, CT9FG, 99.5 -wt% Al₂O₃, Almatis), silicon powder (-325 mesh, 99.5 -wt% Si, Welsch), Aluminium powder (45-75 μm, 99.7 -wt% Al, TLS Technik), Microsilica fume (98.3 -wt% SiO₂, Elkerm), multi-walled CNTs (~50nm, 95 -wt% C, Chengdu Organic Chemicals), Graphite (-200 mesh, 93.0 -wt% C, Fuchs Lubirtech), Phenol Novolak Resin PF6446FL (Co. Hexion) and Carbores^P powder (high melting coal-tar resin, Co. Rütgers) were used as starting materials. The batch composition consisted of 43-wt% 8-14 mesh tabular alumina, 17 -wt% -14 mesh tabular alumina, and 5.0 -wt% calcined alumina. Rest 35 -wt% starting materials consisted of -325 mesh tabular alumina, flake graphite, Al (Si, SiO₂, CNTs) additives. -325 mesh tabular alumina and Al (Si, SiO₂, CNTs) were first hand-mixed for a certain time in a corundum mortar till the colour of mixture looked homogeneous. An extra mixture of 4.0-wt% liquid novolak resin with 0.4-wt% hardener hexa and 2.0-wt% Carbores^P powder was used as bonding system. The whole residual carbon of the sample was set at around 5.0-wt%.

All batches were mixed following the same procedure by Toni mixer and then pressed to bars (25 mm in height, 25 mm in width and 150 mm in length) with the aid of a hydraulic press at a pressure of 150 MPa. Consequently, all the samples were hardened following the

standard temperature-time curve up to 180 °C. Then, the samples were treated at 1200 or 1400 °C in coke grit bed for 3h. The apparent porosity was measured according to EN 933-1. The cold modulus of rupture (CMOR) was measured due to three-point bending test with respect to EN 933-6, and Young's modulus by impulse method according to DIN 51942. The thermal shock resistance was tested according to EN 993-11. Namely, after the temperature has reached 950 °C, bar samples were put into the carbon grit bed and soaked for 30 minutes then cooled down to room temperature in five minutes by compressed air (P=1.0 bar, 100 mm distance between sample surface and spraying nozzle).

The microstructure of the samples was observed via scanning electron microscope (SEM, Philips, XL30ESEM) linked with energy dispersive spectrometer (EDS, EDAX, PHOENIX). Calorimetric signals from phase transformations of coked powder resin, coked Carbores^P powder and CNTs were monitored by differential thermal analyzer (DTA) using SHIMADZU DTA-50 system. Continuous-heating regimes from room temperature to 1173 K with a heating rate of 10 K/min, samples of 30 mg, open wide Al₂O₃ pans in static dried air. For the DTA measurements, powder resin with 10 -wt% hexa was hardened following the standard temperature-time curve up to 180 °C and then coked at 1000 °C for 3 h in coke grit bed. Also Carbores^P powder was coked at 1000 °C for 3 h in coke grit bed. The fracture behaviour was recorded by high speed camera (SpeedCam MacroVis, High Speed Vision Co.) with a CCD resolution of 1280×386 pixels at the speed of 3000 fps.

2.2 Mechanical properties and microstructure

Table 1 shows the main variable compositions, the apparent porosity, CMOR, Young's modulus, and σ/E of different batches. In comparison of Al (AT), Si (BT), and SiO₂ (CT) respectively playing with CNTs after coked at 1200°C, the apparent porosity of all the batches almost was the same. However, CMOR of batch BT was higher than the other two batches, and then batch CT followed. By increasing the treating temperature, the apparent porosity remained almost the same; in contradiction CMOR of BT and CT batches decreased a lot, and only CMOR of batch AT increased. Among these three batches, Young's modulus of batch CT was the lowest, and its ratio of σ/E reached a value of 0.5×10^{-3} after coking at 1200°C. Using combination of Al, Si and CNTs as additives, the apparent porosity of samples was slightly lower than batches AT, BT and CT after coking at 1200°C and 1400°C, respectively; their CMOR and young's modulus were a little higher than those of other batches. Based on the composition of industrial products, a reference batch D was created. Its CMOR and Young's modulus were quite higher than the former batches after coking at 1200°C. Whereas, after coking at 1400°C, the apparent porosity of batch D increased and their CMOR decreased sharply with a high young's modulus.

Our previous research shows that the CMOR of samples with liquid novolak resin binder is lower than that of corresponding samples with Carbores^P (Aneziris et al., 2009). The previous results also show that by using the combination of Al, Si, SiO₂ and CNTs additives, Al₂O₃-C refractories can achieve better mechanical and thermo mechanical properties. Hence this combination was introduced into Al₂O₃-C refractories with carbonaceous resin powder, referred as E series. With the increase of CNTs from zero to 0.5 -wt%, CMOR of the samples after coking at 1200°C reached its maximum as CNTs content was 0.05 -wt%. However, after coked at 1400°C, CMOR of the samples kept close to each other. It is worth noting that Young's modulus of batch E-0.05 was quite close to that of batch E, although CMOR of batch E-0.05 was higher than the latter. σ/E of batch E-0.05 was higher than that of

E, which indicates the samples with all the additives will possess better thermo mechanical properties in terms of thermal shock performance.

Fig.1 shows SEM images of samples with Al and CNT additives, there were a lot of whiskers in the matrix, which were seldom found in the matrix of samples with same additives and powder resin as bonding system (Aneziris et al., 2009). As demonstrating in Fig.2, these whiskers were nanotubes or of submicron size. Al_4C_3 granules were deposited on the surface of whiskers obviously, some of which grew as branches out from the surface of the whiskers. In case of the samples with Si and CNTs additives, nano-sized SiC whiskers were found easily (Fig.3). Compared to the original shape and dimension of CNTs in the samples (Fig.4), it is evident that whiskers in batch AT were much thicker in diameter and in contradiction those in batch BT were thinner. In addition, the surface of all the whiskers in batch AT and BT was quite rough. When SiO_2 was added into Al_2O_3 -C materials with CNTs, only SiO_2 balls coated with SiC layer and honeycomb microstructure were identified in Fig.5, which is similar to the achieved results in the samples with liquid and powder resin binder.

		AT	BT	CT	DT	D	E	ET-0.05	ET-0.1	ET-0.3	ET-0.5
-325mesh tabular alumina		32.6	32.6	32.6	31.1	31.1	29.6	29.6	29.6	29.6	29.6
Al		1.5	-	-	1.5	1.5	1.5	1.5	1.5	1.5	1.5
Si		-	1.5	-	1.5	1.5	1.5	1.5	1.5	1.5	1.5
SiO_2		-	-	1.5	-	-	1.5	1.5	1.5	1.5	1.5
CNTs		0.3	0.3	0.3	0.3	-	-	0.05	0.1	0.3	0.5
Graphite		0.6	0.6	0.6	0.6	0.9	0.9	0.85	0.8	0.6	0.4
1200 °C	Apparent porosity (%)	18	18	19	17	16	15	15	15	16	17
	Cold modulus of rupture (MPa)	6.27	9.30	7.79	9.78	13.40	18.42	19.40	17.66	15.10	11.54
	Young's modulus (GPa)	21.3	23.9	15.8	26.0	33.6	41.0	40.9	37.7	32.8	27.6
	σ/E (10^{-3})	0.3	0.4	0.5	0.4	0.4	0.4	0.5	0.5	0.5	0.4
1400 °C	Apparent porosity (%)	18	17	18	17	19	17	16	16	16	17
	Cold modulus of rupture (MPa)	7.71	7.16	6.97	8.94	8.89	13.30	13.11	13.75	14.41	13.49
	Young's modulus (GPa)	24.8	21.6	20.3	24.7	30.6	39.0	39.7	37.3	33.1	28.4
	σ/E (10^{-3})	0.3	0.3	0.3	0.4	0.3	0.3	0.3	0.4	0.4	0.5

Table 1. Properties among different recipes of Al_2O_3 -C materials prepared by premixing CNTs with fine powders.

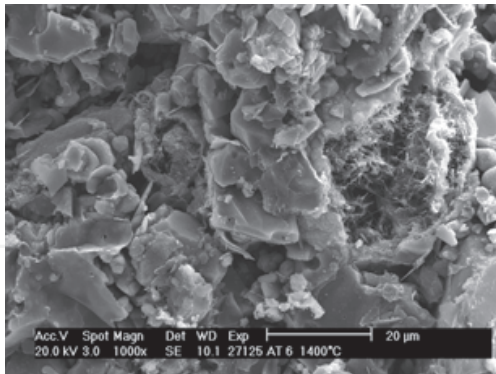


Fig. 1. Microstructure of the sample with Al and CNTs additives, magnification 1000x, coked at 1400°C for 3h.

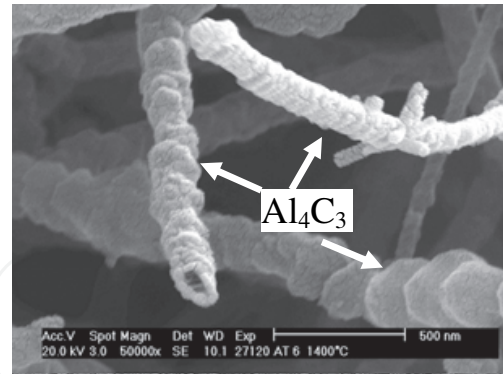


Fig. 2. Microstructure of the sample with Al and CNTs additives, magnification 50000x, coked at 1400°C for 3h.

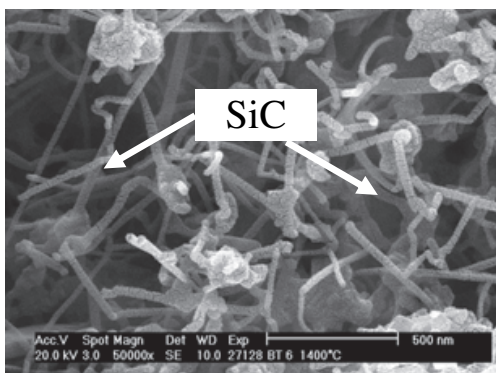


Fig. 3. Microstructure of the sample with Si and CNTs additives, magnification 50000x, coked at 1400°C for 3h.

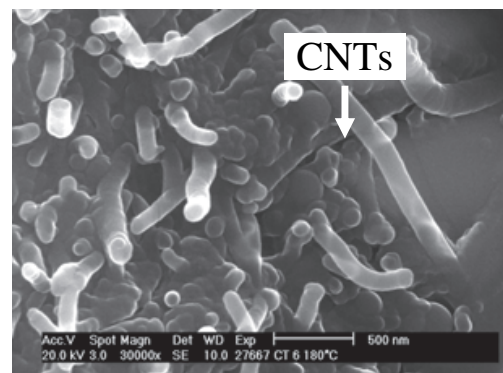


Fig. 4. Microstructure of the sample with SiO₂ and CNTs additives, magnification 30000x, cured at 180°C.

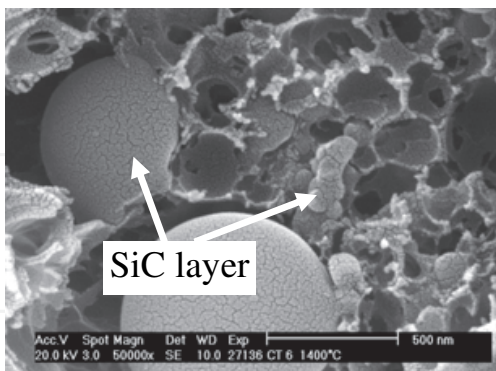


Fig. 5. Microstructure of the sample with SiO₂ and CNTs additives, magnification 50000x, coked at 1400°C for 3h.

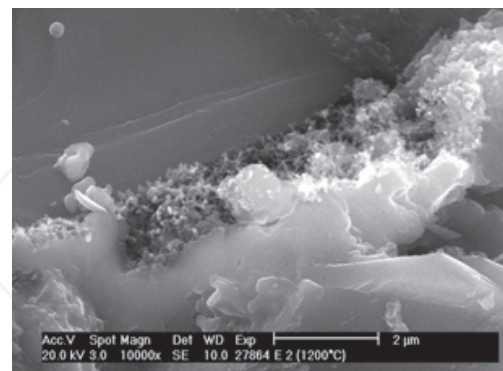


Fig. 6. Microstructure of the sample with Al, Si, and SiO₂ additives, magnification 10000x, coked at 1400°C for 3h.

The samples with Al, Si and SiO₂ additives, fewer amounts of short whiskers were registered between coarse particles and matrix (Fig. 6), compared with the samples with Al and Si additives (Fig.7). In case of the samples with Al, Si, SiO₂ and 0.05-wt% CNTs additives coked at 1200°C, a lot of smoothly nano-sized whiskers were observed, which diameters were less than those of original CNTs (Fig.8). With further enhance of treating temperature, the whiskers became

aggregated and looked inhomogeneous (Fig.9). In addition, an increase of CNTs content in the samples promoted whiskers growth into submicron diameters (Fig.10). It is interesting to observe a lot of CNT-shaped materials still buried in the matrix even after coked at 1400°C (Fig.11), and this phenomenon is hardly seen in the samples with liquid resin and powder resin as binders. Definitely, Carbores^P powder has exerted a particular influence on the microstructure evolution and as a result on the achieved mechanical properties of Al₂O₃-C refractories.

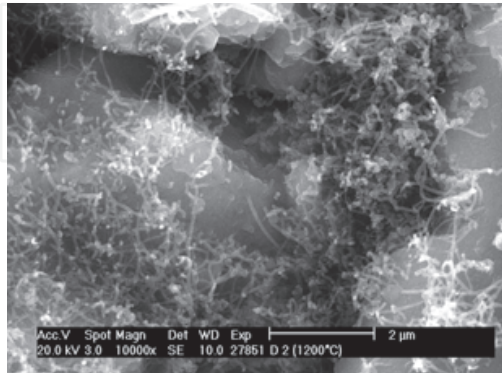


Fig. 7. Microstructure of the sample with Al, Si additives, magnification 10000x, coked at 1400°C for 3h.

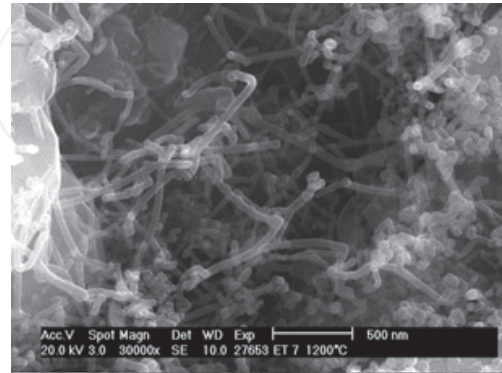


Fig. 8. Microstructure of the sample with Al, Si, SiO₂ and 0.05-wt% CNTs additives, magnification 30000x, coked at 1200°C for 3h.

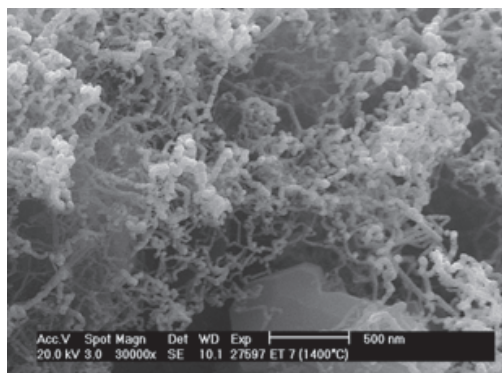


Fig. 9. Microstructure of the sample with Al, Si, SiO₂ and 0.05-wt% CNTs additives, magnification 30000x, coked at 1400°C for 3h.

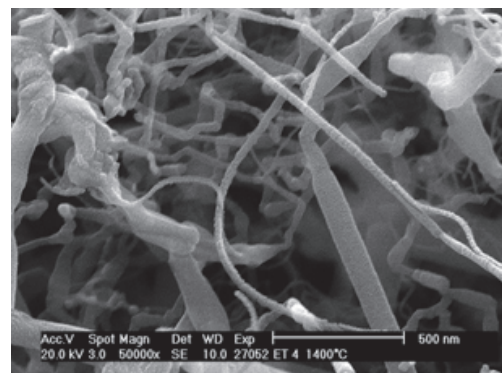


Fig. 10. Microstructure of the sample with Al, Si, SiO₂ and 0.5-wt% CNTs additives, magnification 50000x, coked at 1400°C for 3h.

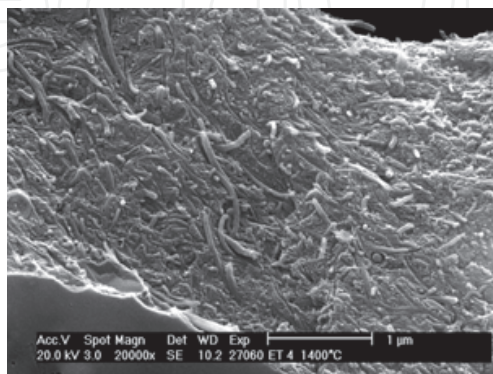


Fig. 11. Microstructure of the sample with Al, Si, SiO₂ and 0.5-wt% CNTs additives, magnification 20000x, coked at 1400°C for 3h.

2.3 Thermal shock resistance and fracture behaviour

Usually, Al and Si are employed in commercial $\text{Al}_2\text{O}_3\text{-C}$ slide gates to improve their mechanical and thermo mechanical properties. Therefore, batch D was chosen as reference to compare its thermal shock performance with those of batch E and E-0.05 (Table 2). After 5 thermal shock cycles, Batch D performed the worst resistance to thermal shock with 48% loss of the CMOR down to 6.95MPa. Batch E and E-0.05 achieved 26% loss in CMOR value. After 5 times thermal shock cycles, E-0.05 still presented a higher CMOR value than E as before thermal shock attack. It is too early to conclude that Batch E is more attractable according to this thermal shock test with the aid of blowing air, due to its low cost without CNTs additive.

After coked at 1200°C	D*	E	E-0.05
CMOR/MPa	6.95	13.60	14.28
Loss in CMOR / %	48	26	26

Table 2. Results of batch D, E and E-0.05 after 5th thermal shock cycles

Three-point bending tests were further performed accompanied by high speed camera records. During the bending test, the initiation of cracks started from the defective places such as scratches, holes or weak bonding positions at the edges of the samples, as shown in Fig.12-14. It is difficult to calculate the propagation length of crack as a function of time step, due to the fact, that the first crack line propagated very fast into the centre. Furthermore, the crack was hardly distinguished due to pictures obtained with the aid of the high speed camera because the surface of samples was rough and relatively dark..

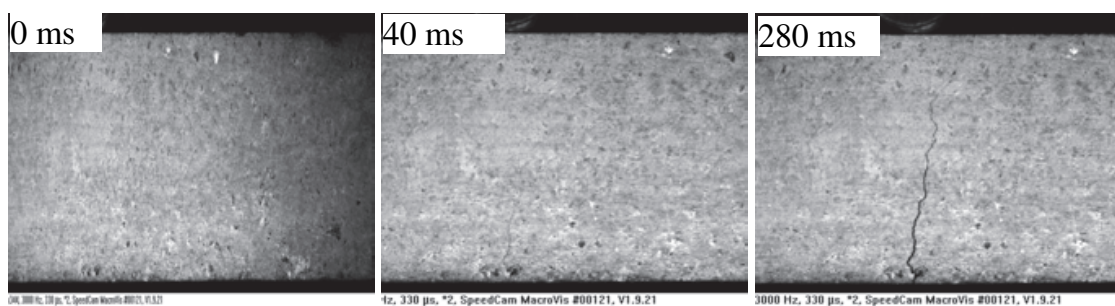


Fig. 12. Fracture evolution of the sample with Al and Si additives after coked at 1200°C for 3h.

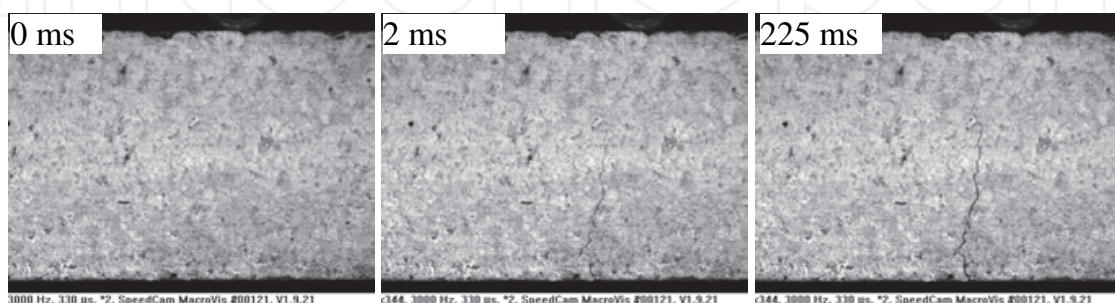


Fig. 13. Fracture evolution of the sample with Al, Si and SiO_2 additives after coked at 1200°C for 3h.



Fig. 14. Fracture evolution of the sample with Al, Si, SiO₂ and CNTs additives after coked at 1200°C for 3h.

According to these observing conditions only two time dependent stages of the crack propagation could be defined. The first stage is before the crack is reaching half of the thickness of the sample, and the second stage before the crack is reaching 3/4 of the thickness of the sample. Correlating the propagation time of the cracks to the real thickness of the samples, propagation velocities were calculated, Table.3. For all samples, the propagation velocities of the first stage were quite higher than these of the second stage. . This phenomenon suggests that propagation of crack in the first stage is very important for understanding and describing the fracture behaviour. During the first stage, batch E presented the highest propagation velocity up to 7.42 m/s. The crack propagating velocity of batch E seems to be related with its microstructure, where whiskers were not contributing to the main bonding reinforcement. In contrast, batch D presented the lowest propagation velocity of crack and batch E-0.05 was in the same order of magnitude to batch D, where a lot of whiskers interlocked the particles and the matrix. Al₂O₃-C refractories working at high temperature as slide gate, endures not only the thermal shock but also the strength from exterior. After service in a certain time, a lot of cracks will be generated. If the resistance to crack propagation is weak, the working safety will lead to total failure of the component.. On the other hand, thermal shock tests of carbon bonded refractories with the aid of blowing air gives insufficient information about crack propagation. Taking into account the propagation velocity and with respect to the CMOR value as coked and after thermal shock, we can assume that batch E presents insufficient service properties during long loading time, and batch E-0.05 achieves excellent mechanical properties.

Coked after 1200°C	Propagation velocity of cracks	
	First stage	Second stage
D	0.32m/s	0.03m/s
E	7.42m/s	0.03m/s
ET-0.05	0.50m/s	0.03m/s

Table 3. Propagation velocities of cracks during bending tests

In order to illustrate the contribution of Carbores^P in Al₂O₃-C materials, the oxidation behaviour of three carbon resources was compared via DTA. Both powder resin with curing agent of hexa and Carbores^P were coked in 1000°C for 3 h before measurement. According to the patterns in Fig.15, the oxidation of the coked powder resin and CNTs were initiated at the temperature around 470°C. However, the slope of DTA curve from CNTs was higher than that of coked powder resin. In addition, the maximum height of DTA curve from CNTs

was larger than that of coke powder resin, which demonstrates the oxidation of CNTs is more intensive than powder resin. In the case of coked powder resin, the oxidation trace was significantly prolonged from 633.34°C to 700.97°C. As for CNTs, except the calometric peak in 662.13°C responsible to the oxidation, another peak in 862.85°C represents the oxidation of the remaining metallic dopant (Illeková & Csomorová, 2005). When coked Carbores^P powder was measured, one endothermic peak was identified at 528.82°C corresponding to softening of Carbores^P; this peak was even registered if Carbores^P powder had been pre-coked at 1000°C for 3h. The oxidation of Carbores^P took place obviously at 672.38°C, and then presented slow oxidation behaviour over 950°C. Carbores^P powder performed the best oxidation resistance among the three carbon resources.

As described by Aneziris et al., Carbores is an environmental friendly artificial tar resin, with a softening point over 200°C (Aneziris et al., 2009; Boenigk et al., 2004). It preserves the characteristic of pitch, which is softening and pyrolyzes in liquid state at higher temperature during heating process, while powder resin pyrolyzes in solid state. This liquid state decreases the oxidation of antioxidants, as well as the oxidation of CNTs wrapped by the liquid, since the oxidation in carbon containing materials is controlled by oxygen diffusion in the decarbonised layer (Simmat et al., 2003). This is the reason that a lot of CNTs still can be found after coked at 1400°C as shown in Fig.9. On the contrary, CNTs can not be observed in the matrix of the samples with liquid and powder resin as binder systems. In one hand, Carbores^P powder improves the mechanical properties by promoting the formation of carbides or nitrides from antioxidants as Al, Si in the Al₂O₃-C refractories due to the liquid state of Carbores^P at elevated temperature. On the other hand, ceramic bonding makes Al₂O₃-C materials much brittle to resist the thermal shock and crack propagation under load, as revealed by batch E in Table 3. Thus the flexible phases such as CNTs are necessary to enhance the integrated service properties of Al₂O₃-C refractories.

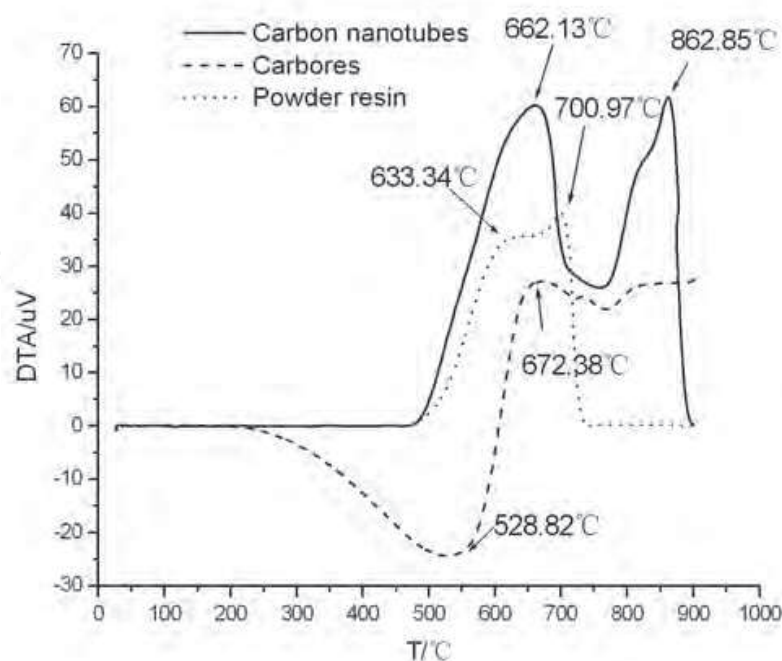


Fig. 15. DTA traces of high temperature oxidation of coked powder resin, coked Carbores and carbon nanotubes at 10K min⁻¹

2.4 Conclusion

Carbonaceous resin powder (Carbores) is well known in carbon containing materials due to not only its environmental friendly but also its improvement on the oxidation resistance and mechanical properties of refractories, compared to liquid and powder resin. Due to the protection based on the Carbores^P -binder system during the heating process, antioxidant Al reacts with CNTs into thicker Al₄C₃ nano or submicron tubes before Al or CNTs are oxidised. Whiskers formed by Si with carbon nanotubes are much thinner than original CNTs, and microsilica fume with a SiC layer is generating anchors and honeycomb microstructures. The combination of additives such as Al, Si, SiO₂ and CNTs enhance the mechanical and thermo mechanical properties, whereby the propagation velocity of the crack is decreased due to the flexibility enforcement by CNTs.

3. Application of CNTs in carbon block for blast furnace

The lifetime of a blast furnace (BF) is decided mainly by the rate of erosion and corrosion of the carbon block in the hearth and bottom area. Currently, carbon block for a BF are being developed with high thermal conductivity and a highly microporous structure. Here, the effect of CNTs addition on the thermal conductivity and porosity characteristics of carbon block for BF is demonstrated. Further considering the cost and dispersion of CNTs, in-situ formation of CNTs in the carbon specimens may be a better choice. In our work, CNTs can be derived from the modified resin containing Ni element, and resin is also one of binders of carbon block. So the effect of the modified resin containing Ni element on the thermal conductivity and porosity characteristics of carbon block is investigated.

3.1 Experimental procedure

Electric-calcined anthracite granules and fine powder (3–5 mm, 1–3 mm, 0–1 mm, and <0.088 mm; Fangda Carbon Co., Ltd., Beijing, China), flaky graphite (<0.075 mm; Qingdao Hengsheng Graphite Co., Ltd., Qingdao, China), brown corundum (<0.075 mm; Zhengzhou Zhenjin Refractory Co., Ltd., Zhengzhou, China), metallic silicon (<0.045 mm; Zhejiang Kaiyuantong Silicon Co., Ltd., Kaiyuan, China), and CNTs (Alpha Nano Tech. Inc., Chengdu, China; diameter: >50 nm, length: ~20 μm, purity: >95 wt%, ash:<1.5 wt%, electrical conductivity:>104 S/m) were used as starting materials. Thermosetting phenolic resin (50 wt% of carbon yield; Yongli Refractory Co., Ltd., Zibo, China) was used as a binder. The chemical composition of all the starting materials is shown in Table 4. The basic recipe contains 66 wt% electric-calcined anthracite, 20 wt% graphite, 6 wt% brown corundum, and 8 wt% Si. CNTs content in the carbon block various from 0.5, 1, 2, 3, 4, to 5 wt%. 11 wt% resin was used as a binder with 5 wt% absolute alcohol. For the homogeneous dispersion of CNTs in the mixture, CNTs were first mixed with resin for 30 minutes with the aid of absolute alcohol. In another experiments, the modified resin containing Ni element as binder was added into the carbon block (2%, 4%, 6%, 8% and 11% respectively). The starting materials were mixed for 30 minutes in a mixer with the rotating speed of 80–100 revolutions per minute. After kneading, cylindrical specimens with 50 mm in diameter and 50 mm in height were pressed under the pressure of 100 MPa. Afterwards the specimens were cured at 110°C and 200°C for 10 hours, respectively, in a muffle furnace. The coking of as-prepared specimens was carried out at 1200°C and 1400°C for 3 hours, respectively, in a crucible filled with industrial carbon grit.

	C	Al ₂ O ₃	SiO ₂	Si	Ash	Volatile	Fe	TiO ₂
electric-calcined anthracite	93	3.87	3.96		7.34	1.35		
Flaky graphite	≥97					1.4		
Brown corundum		≥96	≤0.9				≤0.15	2.5
Metallic silicon				≥98			0.5	

Table 4. Chemical compositions of the raw materials (mass percent)

The bulk density and apparent porosity of the fired specimens were measured. The cold crushing strength was determined in terms of GB/T 2997-85. The micropore size distribution was examined by a mercury porosimeter (Autopore IV9500; Micromeritics Instrument Corp., Norcross, GA). The thermal conductivity was calculated from the product of thermal diffusivity measured using the flash diffusivity technique (Flashline 5000; Anter Corp., Pittsburgh, PA); and heat capacity were also measured. The diffusivity was measured in a direction parallel to the forming direction of the initial carbon block. The samples for cross-sectional analysis were prepared from the fractured specimens and were observed by a field-emission SEM (Nova400 Nano FESEM; FEI Co., Philips', Hillsboro, OR).

3.2 Results and discussion

3.3.1 Effect of CNTs on pore structure and thermal conductivity

A. Pore characteristic and microstructure

Fig. 16 and 17 show the apparent porosity and bulk density of specimens with different CNTs content treated at 1200 °C and 1400 °C in coke bed. The apparent porosities increase and bulk densities decrease with increasing CNTs content. Fig. 18 shows the variations of porosity characteristics. The mean pore diameter for the coked specimens decreases by the addition of 0.5 wt% CNTs, but increases gradually again by subsequent addition of CNTs, e.g., at 1400 °C, from 0.18 μm for 0.5 wt% CNTs to 0.44 μm for 5 wt% CNTs. Meanwhile, the trend of <1 μm pore volume was opposite to that of mean pore diameter, e.g., at 1400 °C, from 80.8 pct for 0.5 wt% CNTs to 66.7 pct for 5 wt% CNTs. As 0.5 wt% CNTs were added, a less amount of CNTs can be dispersed in the matrix easily as filler and can result in an increased particle packing density. The degradation of porosity characteristics by adding CNTs of more than 0.5 wt% may be due to high surface area ratio of CNTs and difficulties in getting a homogeneous dispersion.

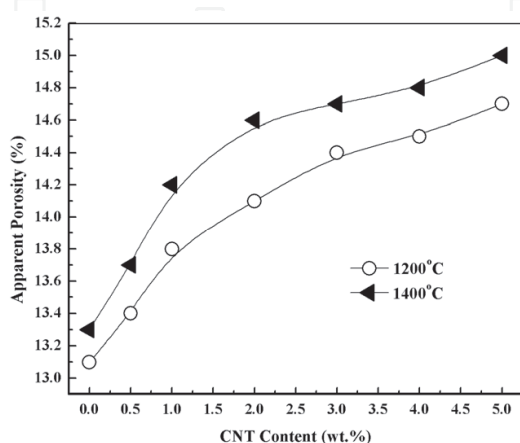


Fig. 16. The variations of apparent porosity as a function of CNT content.

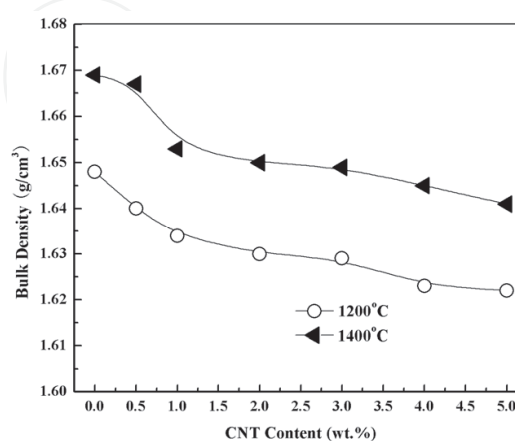
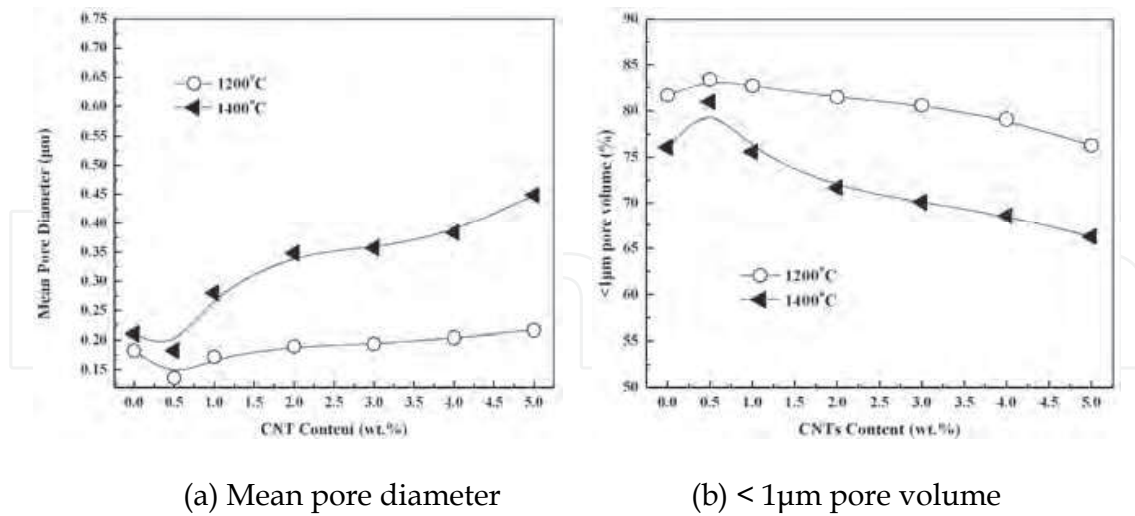


Fig. 17. The variations of bulk density as a function of CNT content.

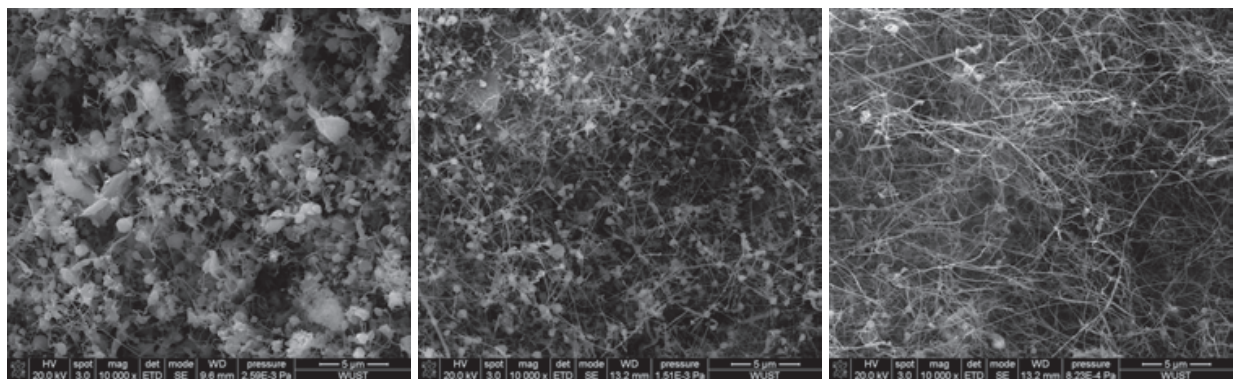


(a) Mean pore diameter

(b) $< 1\mu\text{m}$ pore volume

Fig. 18. The variations of porosity characteristics as a function of CNT content. (a) Mean pore diameter and (b) $< 1\mu\text{m}$ pore volume.

Fig. 19 shows SEM images of fractured specimens with different CNT contents after coking at 1200 °C. For the specimen without CNTs, large amounts of cristobalite particles and SiC whiskers are observed in the matrix with pores (Fig. 16(a)). The amount of cristobalite decreased and SiC increased with the addition of CNT (Fig. 16(b) and (c)), which was attributed to the oxygen partial pressure reduction by adding CNTs. Another notable phenomenon is that the aspect ratio of SiC whiskers became larger with the increased amount of CNTs. From previous work, it was deduced that the pore structures of specimens became worse (Li et al., 2009). Temperature played an important role in the evolutions of cristobalite and SiC whiskers. For the specimens prepared by coking at 1400 °C, the amount of cristobalite decreased and that of SiC increased (Fig. 17), which reveals that the elevated temperature can be favourable for the formation of SiC.



(a)

(b)

(c)

Fig. 16. SEM images of fractured specimens with different CNT contents after coking at 1200°C: (a) 0, (b) 2 wt%, and (c) 5 wt%..

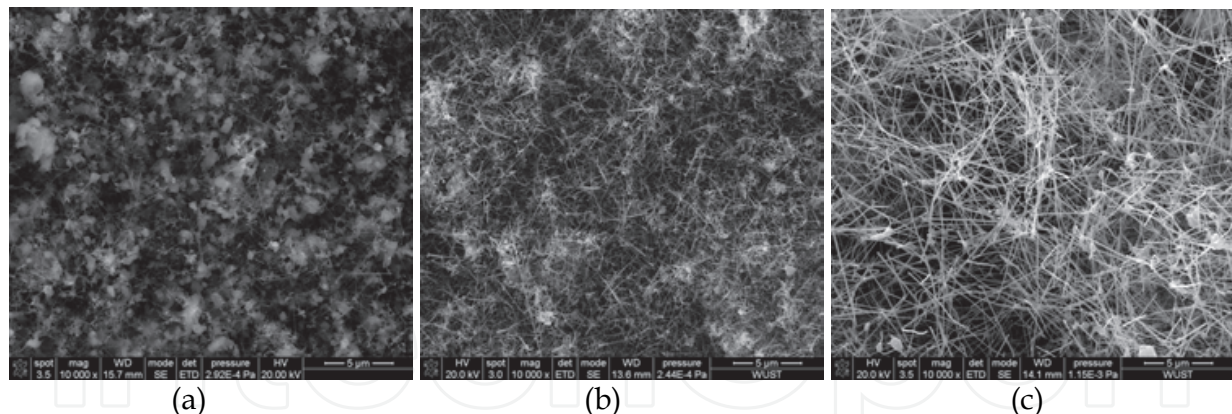


Fig. 17. SEM images of fractured specimens with different CNT contents after coking at 1400 °C: (a) 0, (b) 2 wt%, and (c) 5 wt%.

It was difficult to detect CNTs in the coked specimens. High-magnification SEM indicates that some CNTs were aggregated in the resin locally and were surrounded by graphite flake (Fig.19). Agglomeration observed in coked body resulted from poor dispersion of CNTs during mixing process, which hardly can be avoided because of the high specific surface area of CNTs. It is difficult to achieve a tight interface bonding between the CNTs and the surrounding matrix (Indra et al., 2007; Tsuyohiko et al., 2009), and thus, some CNTs were surrounded by the presence of oxygen. Combined with the previous observations, it can be deduced that the CNTs act as carbon source based on their high reactivity (Emilia & Katarina, 2005) and were consumed by the following reaction during heating process:



It seems that the surrounding atmosphere can produce a significant effect on the survival of CNTs. Under the N_2 (Lim et al., 2005) or vacuum atmosphere (Yeh et al., 2006), CNTs remained intact after the heating treatment. In this work, although the main atmosphere consists of CO and N_2 in theory (Chen, et al., 2008), in fact, locally the oxygen partial pressure is high, especially in the pores and interfaces, plus the high activation of CNTs, and thus CNTs can be consumed easily in increased temperature.

B. Thermal conductivity

The variations of thermal conductivity (25°C) are shown in Fig. 20. The thermal conductivity of the specimens coked at two different temperatures was increased with the increased amount of CNTs up to 4 wt%. For example, at 1400 °C, the thermal conductivity was enhanced from 16.5W/(m·K) for the no CNT specimen to 20.8 W/(m·K) for the 4 wt% CNT specimen, but it decreased slightly again by adding more CNTs. For each carbon specimen, the thermal conductivity of specimens coked at 1400°C was higher than that at 1200°C. The enhancement of thermal conductivity with the addition of CNTs was explained by the increased formation of SiC and the presence of more residual CNTs. The degradation of thermal conductivity by adding CNTs of more than 4 wt% may be attributed to the matrix structure deterioration of coked specimens, which can be shown from the variations in apparent porosity and bulk density. The apparent porosity increased and the bulk density decreased with increasing CNT content. The formation of more interfaces and difficulties in getting a homogeneous CNT dispersion can be responsible for such variations. Indra et al. reported that the interface has a negative effect on thermal conductivity of the composites (Indra et al., 2007). Jiang and

Tsuyohiko et al. found that the homogeneous dispersion of CNTs can increase in the thermal conductivity (Jiang et al., 2008; Tsuyohiko et al., 2009). In our previous work, we found that the high thermal conductivity SiC phase content increased with the coking temperature (Chen et al., 2009), which resulted in the increase of thermal conductivity.

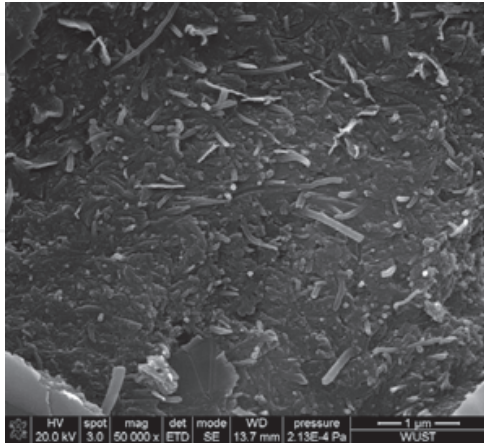


Fig. 19. CNTs in the matrix of specimen with 5% CNTs coked at 1400 °C.

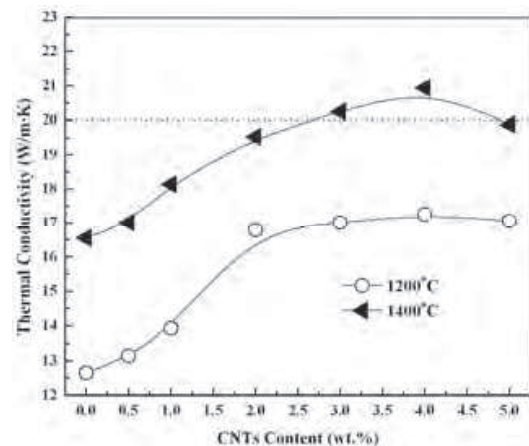


Fig. 20. The variations of thermal conductivity (25 °C) as a function of CNT content.

Theoretically, CNTs can improve the thermal conductivity of coked specimens considerably because of their high thermal conductivity. However, most CNTs were consumed and thus unused, which was contrary to the original expectation. So, how to retain the CNTs intact in the coked specimens is a big challenge. Morisada et al. reported that CNTs can be coated with a SiC layer using SiO vapor in vacuum, thereby enhancing the oxidation resistance of CNTs (Morisada et al., 2004). Liang et al. found that uniform and compact SiC coatings on the surfaces of CNTs can be synthesized in the initial polycarbonsilane/xylene concentration section of 10–15 pct (Liang et al., 2008). Incorporating or in situ forming such CNTs coated with SiC in carbon block may result in the retention of CNTs.

3.3.2 Effect of modified resin on pore structure and thermal conductivity

A. Pore characteristic and microstructure

Fig. 21 shows the mean pore diameter and < 1 μm pore volume of specimens with different modified resin content. The mean pore diameters of specimens treated at 1200 °C have no obvious change, but they increased markedly with increasing of modified resin content at 1400 °C, accordingly, < 1 μm pore volume of specimens decrease evidently.

Fig. 22 shows SEM images of fractured specimens with different modified resin contents. At 1200 °C, there are a great deal of cristobalite particles and SiC whiskers in the specimens; the amount of cristobalite particles also decreased and SiC whiskers increased with the addition of modified resin. Compared with the addition of CNTs, the amount of SiC whiskers are more, and the length/diameter ratio of the whiskers increases. Further observation at high magnification, CNTs are not detected, but a great deal of one dimension of nanoscale fibres/whiskers are easily found in the matrix, just about 10–30 nm in diameter, and mostly composed of carbon with a little Si element. In our previous work, CNTs can be derived by the catalysis of Ni during the process of pyrolysis of modified resin. However, new CNTs have high reaction activity; it is easily oxidised under high oxygen partial pressure conditions in coke bed. In addition, there are 8% silicon in our system, and gaseous substances such as Si(g)

or SiO(g) will occur at high temperature. So the addition of modified resin benefits the formation of SiC whiskers. When the treated temperature is up to 1400 °C, more cristobalite particles occur and just a few SiC whiskers exist in the specimens. At elevated temperature, more gaseous substances are generated, and a part of gaseous substance escape from the inner of specimen, which leads to the apparent porosity increase and the accelerated oxidation of CNTs. This may be the reason for the reduction of whiskers and increase of cristobalite particles obviously.

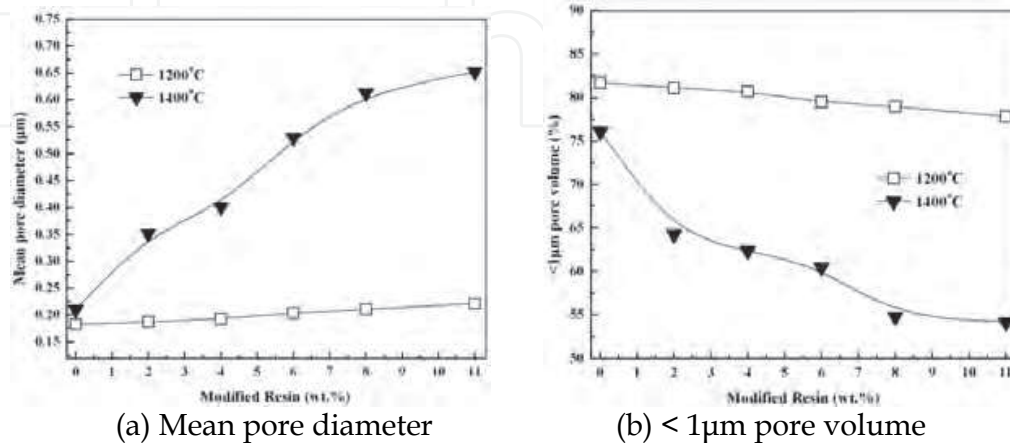


Fig. 21. Mean pore diameter and < 1µm pore volume as a function of modified resin content

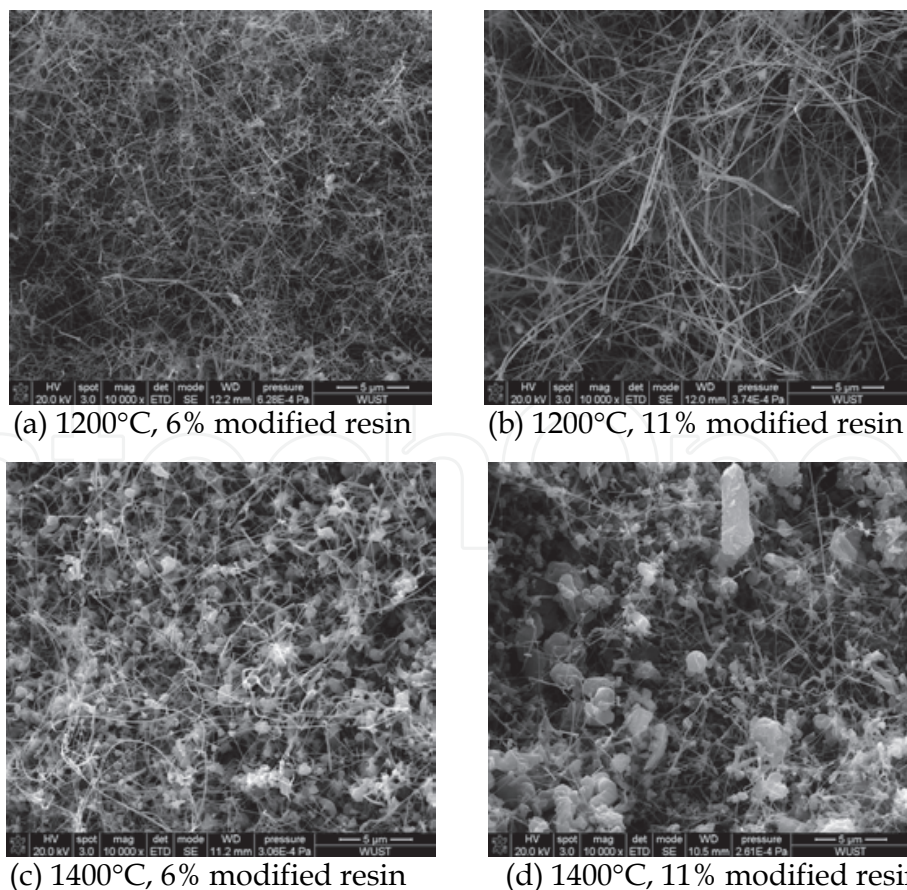


Fig. 22. SEM images of fractured specimens with different modified resin content after coking

B. Thermal conductivity

Fig.23 shows the thermal conductivity of the carbon specimens coked at 1200°C and 1400°C when the modified resin was used. The thermal conductivities at room temperature increased with the addition of modified resin and decreased when the amount of modified resin is bigger than 8%. The thermal conductivity of the specimen with 8 wt% modified resin coked at 1400°C is the largest, approaching to 22.2 W/m·K; compared with no modified resin specimen, it increases by about 30%. From the fracture microstructure of specimens, some fine SiC whiskers or one dimension carbon materials can be easily found in the matrix, and the quantity of SiC whiskers increases with the addition of modified resin. Whether modified resin transforms into CNTs or SiC whiskers, they all enhance thermal conductivity of the specimens. Compared with the direct addition of CNTs, the addition of modified resin is more effective to enhance thermal conductivity. So it is feasible to use modified resin as the binder for improving the thermal conductivity of carbon block.

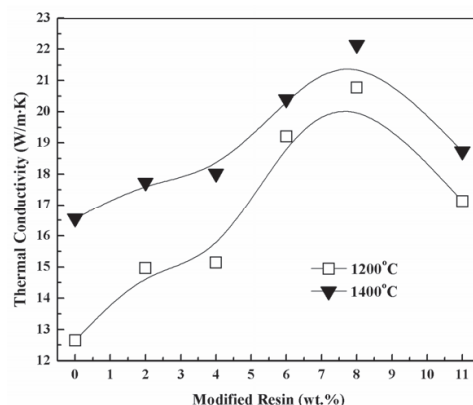


Fig. 23. Thermal conductivity at room temperature changing with addition of modified resin

3.3 Conclusions

The direct addition of CNTs benefits the enhance of the thermal conductivity of carbon block for blast furnace, although just a few CNTs are remaining in the specimens. At high temperature, most of CNTs act as carbon source, react with Si to form SiC whiskers. With the increase of CNTs content, the formation amount of SiC whiskers is increased and their aspect ratio becomes larger, and the SiC whiskers tend to be nonhomogeneously distributed. The thermal conductivity of the carbon specimen containing 4 wt% CNTs is the highest, which can be attributed to the contribution of the SiC whiskers and residual CNTs. However, the excessive addition of CNTs degrades the porosity characteristics. The addition of modified resin also benefits the formation of SiC whiskers, and enhances thermal conductivity more effectively. Considering the cost and dispersion of CNTs, it is feasible to use modified resin as a binder system for improving the thermal conductivity of carbon block.

4. References

- Aneziris, C; Borzov, D. & Ulbricht J. (2003). Magnesia-Carbon bricks-a high duty refractory material, *Interceram- Refractories Manual*, 22-27, ISSN 0020-5214.
- Aneziris, C; Jin, S. & Li, Y. (2009). Interactions of carbon nanotubes in Al₂O₃-C refractories for sliding gate application. *UNITECR'09*, 2009, Brazil.

- Boenigk, W.; Stiegert, J. & Jacob, C. (2004). MgO-C-bricks produced in a cold-mixing process using a graphite forming binder system, *47th Intern. Colloquium on Refractories*, Aachen, 46-51, ISSN 1004-4493.
- Chen, X.; Li, Y. & Li, Y. (2008). Carbothermic reduction synthesis of Ti(C, N) powder in the presence of molten salt. *Ceramics International*, 34: 1253-1259, ISSN 0272-8842.
- Chen, X.; Li, Y. & Li, Y. (2009). Effect of temperature on the properties and microstructures of carbon refractories for blast furnace (BF). *Metallurgical and Materials Transactions A*, 40A, 1675-1683, ISSN 1073-5623.
- Emilia, I. & Katarina, C. (2005). Kinetics of oxidation in various forms of carbon. *Journal of Thermal Analysis and Calorimetry*, 80:103-108, ISSN 1572-8943.
- Illeková, E. & Csomorová, K. (2005). Kinetics of oxidation in various forms of carbon, *J. Thermal Analysis and Calorimetry*, 80: 103-108, ISSN 1418-2874.
- Indra, S.; Masataka, T. & Morinobu, E. (2007). Effect of interface on the thermal conductivity of carbon nanotube composites. *International Journal of Thermal Sciences*, 46: 842-847, ISSN 1290-0729.
- Lim, D.; You, D. & Choi, H. (2005). Effect of carbon nanotube addition on the tribological behavior of carbon/carbon composites. *Wear*, 259: 539-544, ISSN 0043-1648.
- Jiang, L. & Gao, L. (2008). Densified multiwalled carbon nanotubes-titanium nitride composites with enhanced thermal properties. *Ceramics International*, 34: 231-235, ISSN 0272-8842.
- Li, Y.; Chen, X. & Sang, S. (2010). Microstructure and Properties of Carbon Refractories for Blast Furnace with SiO₂- and Al-additions. *Metallurgical and Materials Transactions A*, 41A: 2085-2092, ISSN 1073-5623
- Liang, T.; Zhao, H. & Zhang, Y. (2006). Electromagnetic Wave Absorption Properties of SiC Coated CNTs Nano-composites, *J. Inorg. Mater.*, 21(3): 659-63, ISSN 1000-324X.
- Tsuyohiko, F.; Takahiro, F. & Naotoshi, N. (2009). Evaluation of dispersion state and thermal conductivity measurement of carbon nanotubes/UV-curable resin nanocomposites. *Synthetic Metals*, 159: 827-830, ISSN 0379-6779.
- Morisada, Y.; Maeda, M. & Shibayanagi, T. (2004). Oxidation resistance of multiwalled carbon nanotubes coated with Silicon Carbide. *Journal of the American Ceramic Society*, 87(5): 804 -808, ISSN 0002-7820.
- Simmat, R. & Pötschke, J. (2003). Oxidation experiments on different types of carbon bond of refractories, *Stahl und Eisen Special*, 11-12, ISSN 0340-4803.
- Shadab, S.; Khalid, L. & Edward, S. (2007). The effect of a CNT interface on the thermal resistance of contacting surfaces. *Carbon*, 45: 695-703, ISSN 0008-6223.
- Yeh, K.; Tai, H. & Liu, H. (2006). Mechanical behavior of phenolic-based composites reinforced with multi-walled carbon nanotubes. *Carbon*, 44: 1-9, ISSN 0008-6223.



Carbon Nanotubes Applications on Electron Devices

Edited by Prof. Jose Mauricio Marulanda

ISBN 978-953-307-496-2

Hard cover, 556 pages

Publisher InTech

Published online 01, August, 2011

Published in print edition August, 2011

Carbon nanotubes (CNTs), discovered in 1991, have been a subject of intensive research for a wide range of applications. In the past decades, although carbon nanotubes have undergone massive research, considering the success of silicon, it has, nonetheless, been difficult to appreciate the potential influence of carbon nanotubes in current technology. The main objective of this book is therefore to give a wide variety of possible applications of carbon nanotubes in many industries related to electron device technology. This should allow the user to better appreciate the potential of these innovating nanometer sized materials. Readers of this book should have a good background on electron devices and semiconductor device physics as this book presents excellent results on possible device applications of carbon nanotubes. This book begins with an analysis on fabrication techniques, followed by a study on current models, and it presents a significant amount of work on different devices and applications available to current technology.

How to reference

In order to correctly reference this scholarly work, feel free to copy and paste the following:

Yawei Li, C.G. Aneziris, Shengli Jin, Shaobai Sang and Xilai Chen (2011). Application of Multi-Walled Carbon Nanotubes for Innovation in Advanced Refractories, Carbon Nanotubes Applications on Electron Devices, Prof. Jose Mauricio Marulanda (Ed.), ISBN: 978-953-307-496-2, InTech, Available from:
<http://www.intechopen.com/books/carbon-nanotubes-applications-on-electron-devices/application-of-multi-walled-carbon-nanotubes-for-innovation-in-advanced-refractories>

INTECH
open science | open minds

InTech Europe

University Campus STeP Ri
Slavka Krautzeka 83/A
51000 Rijeka, Croatia
Phone: +385 (51) 770 447
Fax: +385 (51) 686 166
www.intechopen.com

InTech China

Unit 405, Office Block, Hotel Equatorial Shanghai
No.65, Yan An Road (West), Shanghai, 200040, China
中国上海市延安西路65号上海国际贵都大饭店办公楼405单元
Phone: +86-21-62489820
Fax: +86-21-62489821

© 2011 The Author(s). Licensee IntechOpen. This chapter is distributed under the terms of the [Creative Commons Attribution-NonCommercial-ShareAlike-3.0 License](#), which permits use, distribution and reproduction for non-commercial purposes, provided the original is properly cited and derivative works building on this content are distributed under the same license.

IntechOpen

IntechOpen